

# Numerical Modelling of Slip-Resistant Stainless Steel Bolted Connections

*Anqi Chen<sup>a</sup>, Petr Hradil<sup>b</sup>, Timo Manninen<sup>c</sup> & Nancy Baddoo<sup>a</sup>*

*The Steel Construction Institute, Ascot, UK<sup>(a)</sup>*

*VTT, Technical Research Centre of Finland, Espoo, Finland<sup>(b)</sup>*

*Outokumpu Stainless Oy, Tornio Research Centre, Tornio, Finland<sup>(c)</sup>*

## Abstract

The use of stainless steel in building construction has become more popular in recent years. It is used for a wide range of structural applications in aggressive environments where reliable performance over long periods with little maintenance is required. Although structural design standards are available for stainless steel, currently there are no rules covering the design of preloaded slip-resistant bolted connections because of the lack of knowledge about their long-term viscoplastic behaviour. Viscoplastic creep and stress relaxation in the preloaded bolt assemblies will lead to certain loss of clamping force and may cause the failure of the connection if it is not accounted for. This paper presents the development of material models and finite element models of bolt assemblies based on the extensive experimental study of the creep, relaxation and tension at different loading rates of austenitic, ferritic, duplex and lean duplex steel plates and bars. These models were verified against slip-tests with stainless steel bolt assemblies according to EN 1090-2 and then used in a parametric study to extend the scope of the investigated connections. Both experimental programmes were carried out in the European RFCS research project SIROCO (Execution and reliability of slip resistant connections for steel structures using carbon steel and stainless steel) as well as the finite element calculations.

## Keywords

Stainless steel, bolts, slip-resistant connections, finite element analysis, preloading, Abaqus, viscoplasticity, creep, relaxations.

## 1 Introduction

Bolted connections are a very convenient joining method in steel structures. They combine the advantages of simple assembly and disassembly together with a high load-carrying capacity. Appropriate preloading methods can further improve their performance and will guarantee the transfer of shear through the friction surfaces rather than the contact between bolt shank and hole. However, design of preloaded bolted connections made from stainless steel can be challenging due to the viscoplastic behaviour of the material, and there is currently no standardized design procedure for stainless steel slip-critical connections. Despite concerns about the loss of clamping force, stainless steel preloaded bolts perform well under static and cyclic loading<sup>[1]</sup>. Their loss of preload in standardized creep tests is comparable to that which occurs in a carbon steel bolted assembly and reliable slip factors can be achieved with a simple surface treatment<sup>[2]</sup>.

Numerical models of bolted connections can be very complex in terms of geometry and interactions between different components of the bolt assembly. Therefore, a wide variety of modelling approaches exist to predict the connection behaviour ranging from simple beam or shell elements to full solid models with detailed threads and contacts definitions<sup>[3]</sup>. Three-dimensional solid models can, in principle, be used to calculate any assembly under any type of loading, but they are the most computationally demanding choice.

This paper presents the development of a computationally efficient numerical model that is practical for use in parametric studies and possible engineering applications in the future. A large part of the effort was focused on possible model simplifications in terms of loading (e.g. avoid the need to rotate the nut), reduced dimensionality (e.g. 2D axisymmetric models), number of elements (e.g. optimized meshing algorithms) and calculation time increments, whilst still obtaining a reliable prediction of the creep and relaxation effect in stainless steel bolts and plates. The characteristics of stainless steel resulted in rather complex material definitions that had to be implemented by FORTRAN user subroutines in Abaqus. It was impossible to provide generic material parameters from the limited experimental data, but the models of several commonly used stainless steel grades are presented in this paper and verified against experiments.

## 2 Strain Rate Dependent Material Definition

According to the literature study<sup>[4]</sup>, only primary creep is observed at room temperature with a limiting minimum stress needed for the creep deformation to occur. This limiting stress increases with work hardening during plastic deformation. The rate of creep deformation depends on the difference between the current stress and stress limit, and on the rate of work hardening in the material. It was also noticed that the creep deformation causes the yield surface to undergo kinematic hardening with an insignificant amount of isotropic hardening<sup>[5]</sup>.

Based on this literature review, the Chaboche model<sup>[6]</sup> was selected for modelling creep of plate materials and later also adapted for bolts and nuts. This model was developed especially for high temperature creep, but nowadays is widely used for modelling cyclic plasticity including room temperature creep of stainless steel. The rate of equivalent (cumulated)

plastic strain  $\bar{\varepsilon}_p$  in the Chaboche material model is given by a power law viscosity function in Eq. 1 with three parameters  $k$ ,  $D$  and  $n$ , and two internal state variables  $\alpha$  and  $R$  to describe the material hardening behaviour:

$$\dot{\bar{\varepsilon}}_p = \left\langle \frac{f(\sigma - \alpha) - R - k}{D} \right\rangle^n \quad (1)$$

where  $f$  denotes the Mises yield function and the Macaulay brackets  $\langle \cdot \rangle$  guarantee that there exists an elastic limit below, which no inelastic deformation occurs. A tensorial back-stress  $\alpha$  describes kinematic hardening of the material in Eq. 2, while the isotropic hardening law in Eq. 3 presents the evolution of drag stress  $R$ :

$$\alpha = \sum_{i=1}^N \alpha_i \quad \text{with the evolution of back-stress components } \dot{\alpha}_i = \frac{2}{3} C_i \dot{\bar{\varepsilon}}_p - \gamma_i \alpha_i \dot{\bar{\varepsilon}}_p \quad (2)$$

$$\dot{R} = b(Q - R) \dot{\bar{\varepsilon}}_p \quad (3)$$

where the rate of plastic strain tensor  $\varepsilon_p$  describes the plastic flow, and constants  $C_i$ ,  $\gamma_i$ ,  $Q$  and  $b$  are additional material parameters to be identified.

The finite element model (FEM) calculations of the bolt assembly showed the best performance when the Chaboche model was used for bolts and plates. Unfortunately, the full set of experiments needed to identify the model parameters was available only for stainless steel plates, while the material for bolts were tested only in simple tension and relaxation. Therefore, a different material model was developed specifically for the bolts which would be mostly subjected to relaxation during the service life of the bolted connection. This simple strain-hardening model is based on relaxation tests carried out at Outokumpu's Avesta Research Centre<sup>[7]</sup> and the calculation of the creep strain  $\varepsilon_v$  is shown in Eq. 4 with parameters  $a$ ,  $b$  and  $c$ , while the time independent plastic strain is modelled as a classic metal plasticity based on the tensile tests.

$$\dot{\varepsilon}_v = c \left[ \frac{\varepsilon_v(1-b)}{c} + a^{1-b} \right]^{\frac{b}{b-1}} \quad (4)$$

It should be noted that the parameter  $c$  depends on the initial stress of the relaxation test and was calibrated either as linear or parabolic fit to this value.

## 2.1 Stainless steel plates

Identification of parameters of mixed kinematic and isotropic hardening models typically require tests with the reversed direction of loading, however, these tests were not carried out in our study. It is well known that the transition from purely kinematic hardening to combined isotropic and kinematic hardening takes place at approximately 1% plastic strain in most engineering materials. Therefore, it was assumed that the rate independent hardening is purely kinematic hardening until the transition point at 1% plastic strain. After this transition point, the observed hardening was divided using a constant ratio of kinematic hardening and isotropic hardening components. For single-phase austenitic and ferritic plate materials, it was assumed that the hardening consists of 60% kinematic hardening and 40% isotropic hardening. For the duplex materials, the hardening was purely isotropic after the transition point.

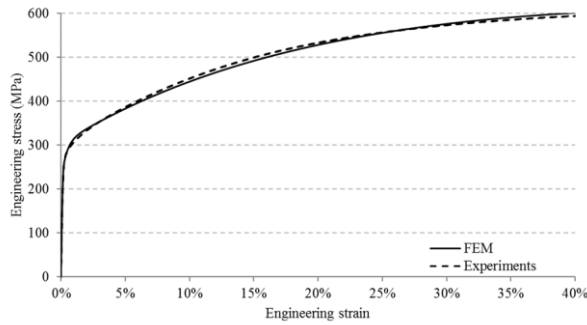
**Table 1** Parameters of Chaboche material model of plates identified from tensile and creep tests

Grade	$k$ (MPa)	$D$ (MPa)	$n$	$Q$ (MPa)	$b$	$C_1$ (MPa)	$\gamma_1$	$C_2$ (MPa)	$\gamma_2$	$C_3$ (MPa)	$\gamma_3$
EN 1.4404 austenitic	73	110	15.0	380	2.5	45949	591.4	617031	6765.3	1434	2.5
EN 1.4003 ferritic	106	130	11.0	104	10.8	623733	5855.1	17430	558.6	1680	10.8
EN 1.4462 duplex	106	313	24.3	723	2.8	947349	1334.6	252038	1222.1	2971	60.0
EN 1.4162 lean duplex	109	329	30.2	649	3.5	483769	4875	102445	975.3	6766	180.8

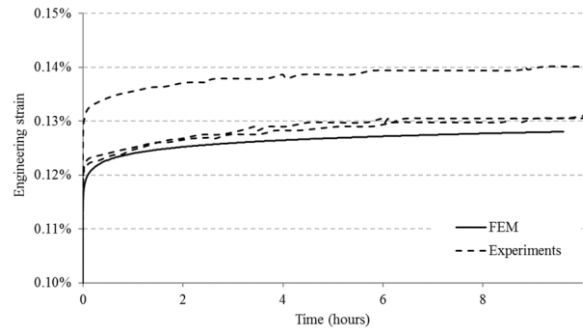
The material parameters for plates made of four different stainless steel grades were identified based on tensile tests with different constant loading rates and creep tests with different stress levels<sup>[5]</sup>. Their values are presented in Table 1.

It should be noted that the inelastic strains are expected to remain below the transition point in the present application. However, the constitutive model represents the whole range of strains observed in the uniaxial tensile test, and therefore is able to provide reliable results in the cases with localized stress concentration in the finite element model.

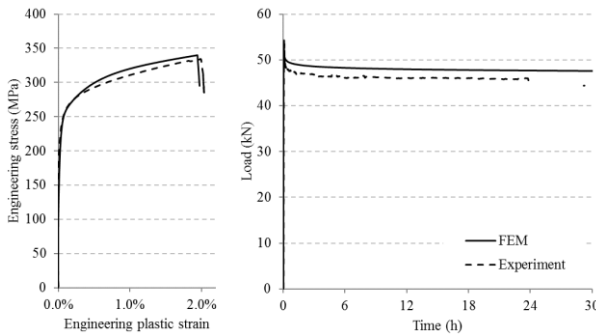
The material behaviour was calibrated against a large test series of stainless steel plates in tension with variable constant loading rate (three tests for each of six rates from  $1 \times 10^{-2} \text{ s}^{-1}$  to  $1 \times 10^{-7} \text{ s}^{-1}$ ) and creep with variable constant load (three tests for each of six loads from: 84 MPa to 336 MPa). The implementation of the material definition in finite element models was then validated against those experiments and additional relaxation tests with variable constant strain (five tests for strains from 0.09% to 2.17%). The material behaviour during loading, constant stress and constant strain was tested on a single finite element model and the examples of the results are presented in Fig 1a (tensile test), Fig 1b (creep test) and Fig 1c (relaxation test including the loading phase).



(a) Tensile test at strain rate of  $1 \times 10^{-4} \text{ s}^{-1}$



(b) Creep test of specimen loaded to 180 MPa



(c) Relaxation test at strain level 2.17%

**Fig 1 Example of validation of the material against material tests**

The finite element model was able to predict accurately tensile loading of the material up to 40% strain for all six levels of loading rate (see example in Fig 1a). The creep tests showed larger scatter, but the finite element prediction of engineering strain remained within the tested range or slightly below it as shown in Fig 1b. Therefore, it was concluded that the accuracy of the model is sufficient for the implementation in FEM. Surprisingly, the validation showed also very good agreement with relaxation tests that were not used for the model calibration (see Fig 1c). The accurate prediction of the material behaviour at constant strain is more important in models of bolt assemblies where the deformation of plates is usually very small.

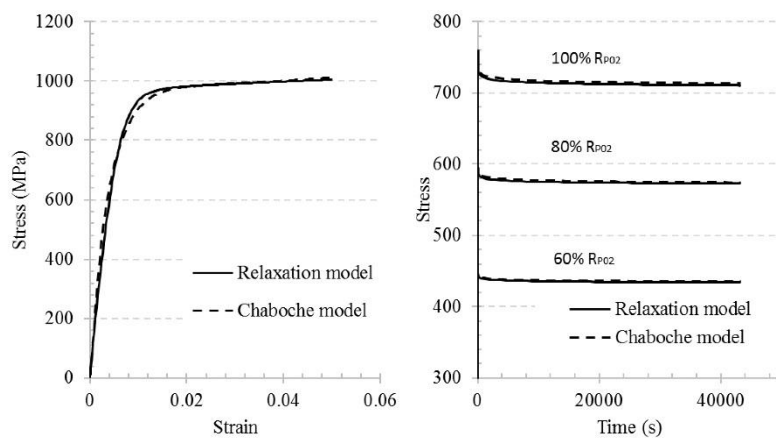
## 2.2 Stainless steel bolts

This strain hardening type model from Eq. 4 was fitted to relaxation tests of austenitic (EN 1.4401), lean duplex (EN 1.4162) and duplex (EN 1.4462) steel bars. This relaxation model was implemented by CREEP subroutine in ABAQUS using static creep analysis. The constitutive model describing the plastic yielding of the stainless steel bolt material is a simple multilinear piecewise isotropic hardening model.

The above material model was developed with the intention of utilising the relaxation test results available from Outokumpu<sup>[7]</sup>. However, its implementation is relatively slow and therefore not suitable for a parametric study. As such, the unified Chaboche model used for plate material was adopted here for the bolt. Parameter identifications were carried out by trial and error using assumed initial values, calibrated solely against the above strain hardening creep model with multilinear plasticity. Table 2 presents Chaboche parameters identified for the bolt material. As an example, a comparison of the relaxation and Chaboche model for austenitic bolt material is shown in Fig 2. It can be seen that the stress-strain and stress relaxation curves are all in excellent agreement. The advantage of having both models are that the relaxation model can utilise readily available stress relaxation data while the calibrated Chaboche model is more computationally efficient.

**Table 2** Parameters of Chaboche model of bolts identified from strain hardening model defined in Eq. 4

Grade	$k$ (MPa)	$D$ (MPa)	$n$	$Q$ (MPa)	$b$	$C_1$ (MPa)	$\gamma_1$	$C_2$ (MPa)	$\gamma_2$	$C_3$ (MPa)	$\gamma_3$
EN 1.4436 austenitic	348.0	200.0	12.0	348.0	1.0	124738.9	320.2	269288.0	2081.2	595.1	1.0
EN 1.4462 duplex	248.0	1133.0	5.13	269.7	1.0	124738.9	320.2	379288.0	2081.2	10.0	1.0
EN 1.4162 lean duplex	298.0	290.0	9.67	269.7	1.0	124738.9	320.2	379288.0	2081.2	10.0	1.0

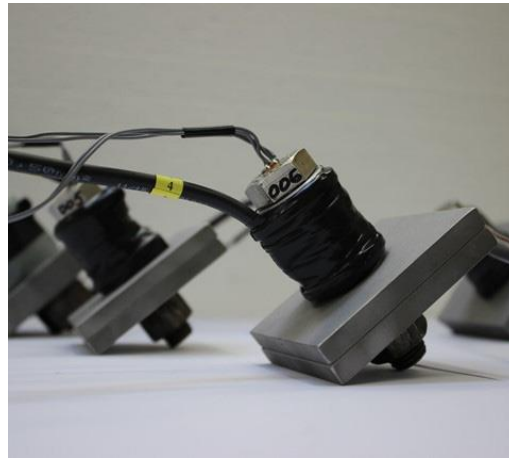
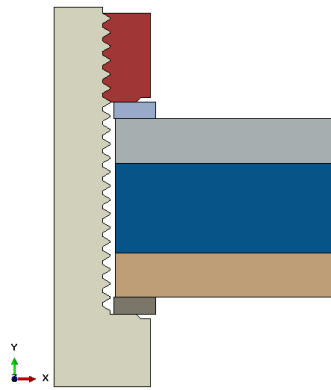
**Fig 2** Comparison of Chaboche and strain hardening relaxation model for austenitic 1.4436 bolt material

### 3 Finite Element Models

The finite element models presented in this paper were developed to simulate the behaviour of the bolt assembly with preloaded stainless steel bolts and rate-dependent material plasticity. The goal was to create optimal models which produce accurate results within a reasonable solution time. The models were constructed using Python script<sup>[8]</sup> developed for the purpose of model calibration and parametric study using ABAQUS<sup>[9]</sup>. The definition of the rate-dependent material hardening (the Chaboche model) was implemented using the FORTRAN subroutine UHARD. The script is executed as a Plug-in in ABAQUS CAE<sup>[5]</sup> and is able to create models using ABAQUS libraries, execute the calculation using the implicit static solver and then evaluate the results if requested.

#### 3.1 Geometry and mesh

The simplest representation of the bolt assembly is a 2D axisymmetric model as shown in Fig 3. It was used for simulation of relaxation of the bolt preload due to material creep of stainless steel at room temperature. However, the 2D model is not sufficient for simulation of slip load and therefore a 3D model of bolted assemblies was developed. The 3D models of the bolt were generated by revolution of the existing 2D axisymmetric bolt model with parallel threads instead of more realistic helical threads modelled in [10]. Even though the 3D helical threads are the most accurate representation of the real bolt, the models were also extremely computationally demanding. These models may be useful in different numerical studies focusing on the tightening phase, where the load can be introduced by the rotation of the nut. The current study, however, used on the simpler 3D model with parallel threads because the effect of thread slope on the loss of preloading force during the lifetime of the structure is negligible<sup>[5]</sup>.

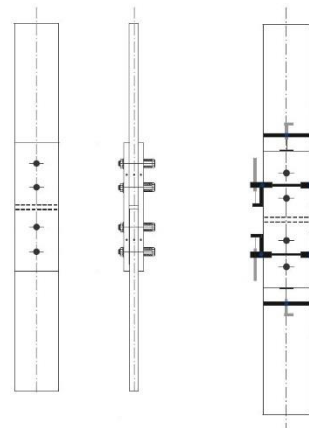
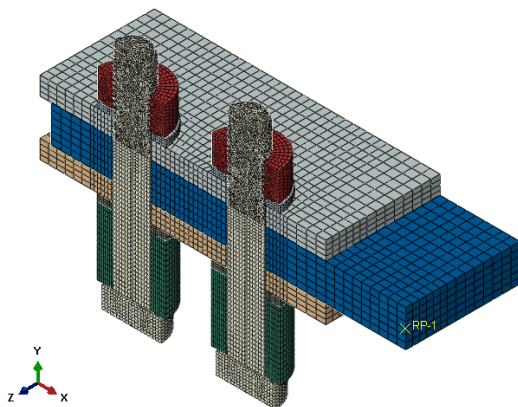


(a) 2D axial symmetric model for bolt load relaxation

(b) Bolt load relaxation test at UDE<sup>[30]</sup>

**Fig 3 2D axisymmetric model and bolt load relaxation test set-up**

Optimised mesh density and use of symmetry planes can greatly reduce the computational time the 3D finite element model. A 3D model of the slip factor test of preloaded M16 bolt assembly according to EN 1090-2 Annex G is shown in Fig 4. The mesh density is finer in the areas with expected stress concentrations and coarse regular mesh is used in other areas. One quarter of the test specimen is modelled due to the double symmetry of the assembly. Load cells were used in the test to monitor the bolt preload so that the clamping length of the test and models are greater than specified in EN 1090-2 Annex G.



(a) 1/4 symmetric finite element model

(b) Experiment set-up using M16 bolts

**Fig 4 3D numerical model for slip factor tests (M16 bolt) according to EN 1090-2 Annex G**

### 3.2 Contact behaviour

Interactions have to be defined between the components for the 3D model shown in Fig 4 in order to properly function. Surface-to-surface interactions were created between cover and centre plates, washers and cover plates, bolt head/nut and washers and the bolt and nut thread. Shear slip resistance of the bolted assembly and preloading in the bolt require contact behaviour to be established in both the tangential and normal direction between all interfaces.

Default “hard” contact normal behaviour was used between all interacting surfaces which minimises the penetration of the slave surface into the master surface and does not allow the transfer of tensile stress across the interface. Separation after contact was allowed so that the faying surfaces were able to separate due to contraction of the plates under shear loading.

Penalty tangential behaviour was defined for modelling the slip and shear load. For simplicity, a friction coefficient of 0.5 was assumed for the interface between the washers and cover plates, bolt head/nut and washers and bolt and nut thread, as they are not the main contributor to the slip resistance of the bolted assembly. The slip behaviour of the joint is mainly dependent on the friction and slip between the faying surfaces of the plates so that the coefficient of friction has to be calibrated against the actual slip test in [29] of different surface preparation process (shot blasted, grit blasted and brushed, etc.).

### 3.3 Material model

The rate-dependent plasticity model (Chaboche model) of plate and bolt materials were implemented using UHARD subroutine in ABAQUS. Parameters of the Chaboche model for each stainless steel type tested are listed in Table 1 and Table 2 above. For simplicity, the washers and load cells were assumed to be elastic only.

### 3.4 Loading

The service life of a connection can be up to 100 years according to Eurocode 0<sup>[12]</sup>. For such long duration, it is not necessary to introduce preload by rotation of nut. The 2D and 3D finite element model were preloaded by reducing the length of bolt shank at the central section in the first step. The displacement of the loaded section plane of the bolt was then remained constant in the second step. For the 2D axisymmetric model, the second step was for bolt load relaxation so no additional load or displacement was applied. However, in order to simulate the slip factor tests, a shear displacement at the end of the central plate was applied in the second step of the 3D model.

The most significant problem with a non-linear solver and numerous contact is the convergence of the calculation. To provide a converging solution, the bolt models had to be loaded with displacement even though the design load typically takes the form of axial force or stress. Unfortunately, it is impossible to predict accurately the required displacement in models with viscoplastic materials, and therefore two solutions were proposed: (1) preliminary analysis with overloaded assembly to determine the displacement (reduction of bolt shank length) – load relation, and (2) indirect monitoring the bolt preload through contact pressure by using the UAMP subroutine.

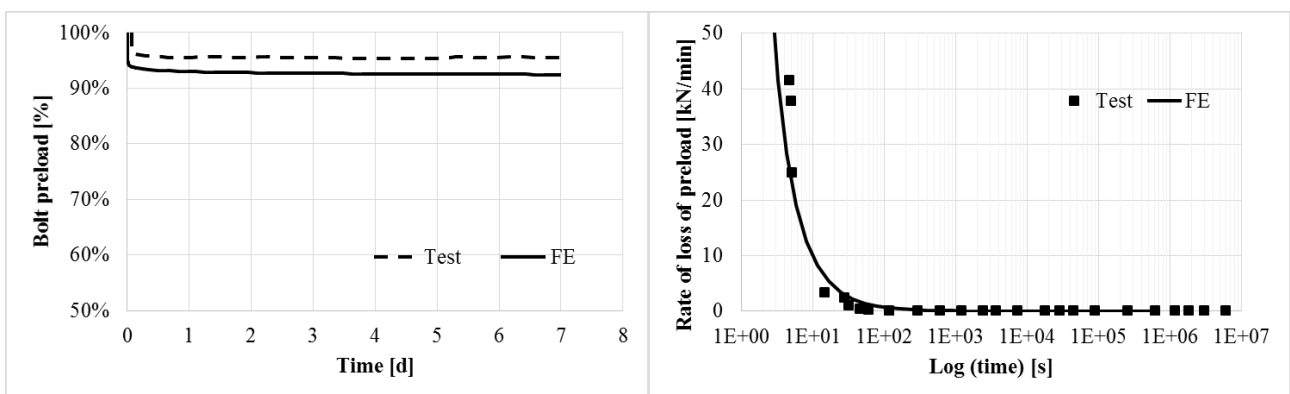
The obvious drawback of the first method is the necessity of one additional preload calculation prior to the actual two-step simulation. Although it does provides an accurate level of displacement hence correct preload in the bolt if the results of the pre-calculation is interpolated correctly, it is not efficient to be used for parametric study. The indirect monitoring of preload should be more efficient. The subroutine is able to terminate the preload calculation step after the first increment with higher contact force (i.e. bolt load) than the design value, and start the second step for relaxation or slip load automatically.

## 4 Validation and Application of Numerical Models

The 2D and 3D models developed in the current study were validated and calibrated using bolt load relaxation tests in [29] and slip factor tests in [30] using stainless steel bolts and plates with various surface finishes. Exemplary simulations of the bolt load relaxation test and slip test to determine slip factors and calibration of friction coefficients are presented in this paper, followed by a parametric study exploring the effect of bolt hole size, preload level, plate thickness and bolt size on slip factors.

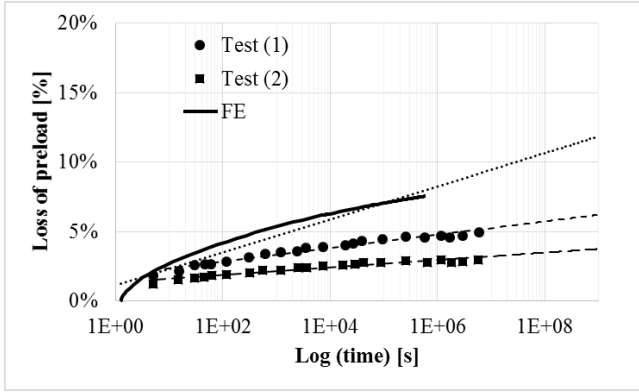
### 4.1 Validation of bolt load relaxation model

It has been shown previously that the Chaboche models are capable of predicting the creep and stress relaxation of various stainless steel bolt and plate material. A large number of bolt load relaxation tests have been carried out in [29]. The 2D axisymmetric model with Chaboche material models was used to predict the bolt load relaxation in stainless steel bolt assembly. A comparison of the loss of bolt preload over a period of 7 days is shown in Fig 5. The single bolt assembly consists of a M20 austenitic bolt and ferritic plates of 75 mm wide and long (similar to the test set-up shown in Fig 3b).



(a) Time history of bolt preload relaxation

(b) Rate of loss of preload



(c) Total loss of preload

**Fig 5 Comparison of bolt load relaxation test using 2D axisymmetric model (M20 austenitic bolts with ferritic plates<sup>[30]</sup>)**

The numerical model accurately reproduces the behaviour that most of the bolt load relaxation occurred at the beginning of the test immediately after preloading, although it slightly over predicted the loss of bolt preload by 2-3% at end of the 7-day period. The rate of loss of preload is however accurately predicted by the numerical model as shown in Fig 5b, where the rate of loss of preload was at a maximum during the first 100 seconds. Fig 5c presents the linear extrapolation of the test and numerical results to 10 years. The numerical model is shown to be more conservative than the test results.

## 4.2 Validation and calibration of slip factor test model

Tests to determine slip factors according to EN 1090-2 Annex G were carried out for different types of stainless steel with shot and grit blasted surface treatment<sup>[29]</sup>. In order to accommodate a load cell for monitoring the bolt load during the test, the clamping length of the tests is greater than it is specified in the standard. A greater clamping length usually leads to a slightly higher slip factor. Slip tests covered austenitic, ferritic, duplex and lean duplex plates with Bumax 88 and 109 (M16 austenitic) bolts. Slip factors were determined for various surface finishes including 1D, shot and grit blasted. The present paper shows the calibration of the numerical model for all slip factor tests in [29]. The 3D model shown in Fig 4 to model only one quarter of the test specimen was used. Chaboche material models were used for both the plate and bolt materials shown in Table 1 and 2 respectively. Nuts were assigned the same material model as bolts while washers were assumed to be elastic only.

The static coefficient of friction for the plate to plate contact behaviour of the numerical model was determined. A comparison of the load – slip displacement curves produced by the tests and the calibrated numerical model is shown in Fig 6, for an assembly of grit blasted austenitic plates with Bumax 88 austenitic bolts. The initial, actual and nominal slip factors are calculated from the slip force  $F_{Si}$  and clamping force  $F_{p,C}$  as shown in Eqn. 5 below:

$$\begin{aligned}\mu_{i,ini} &= \frac{F_{Si}}{4F_{p,C,ini}} \\ \mu_{i,act} &= \frac{F_{Si}}{4F_{p,C,act}} \\ \mu_{i,nom} &= \frac{F_{Si}}{4F_{p,C}}\end{aligned}\tag{5}$$

The friction coefficient of 0.64 was determined so that the nominal slip factor produced by the numerical model is equivalent to 0.57, which is the average value of nominal slip factors produced by four slip tests (eight slip factors generated). It is shown in Fig 6 that the general slip behaviour and loss of preload of the numerical model is in good agreement with tests results.

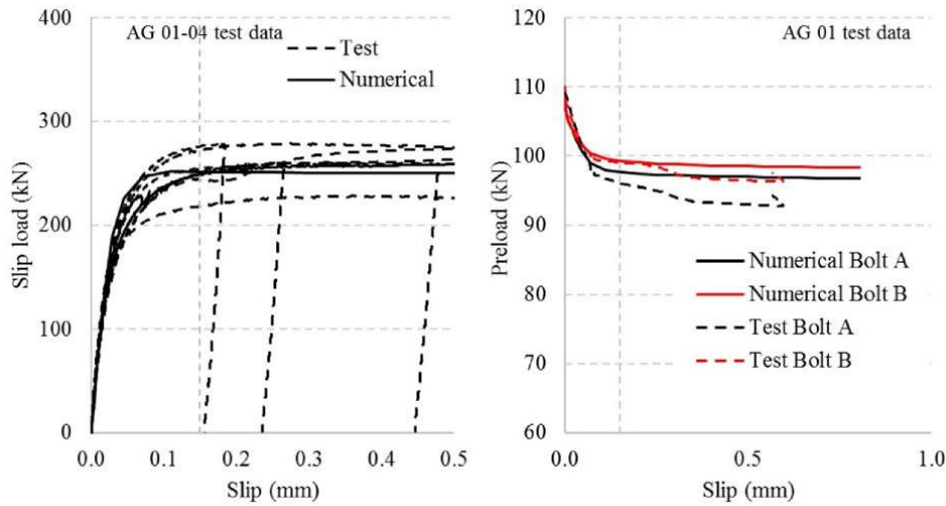


**Fig 6 Calibration of 3D numerical model and comparison with static slip test results: slip-displacement curves (left) and loss of preload (right): Bumax 88 M16 austenitic bolts with grit blasted austenitic plates**

The numerical model was calibrated with all available tests results for different stainless steel bolt and plate material, and surface finishes of the plates. The calibrated numerical results are compared with test data in Table 3. As discussed above, the static coefficient of friction  $\mu_s$  was obtained when the nominal slip factors produced by the numerical models equal the test values. It can be seen that the initial and actual slip factors are also in reasonable good agreement as well.

**Table 3 Results of numerical models validation for all surfaces, bolt and plate material types tested in [30]**

Test ID	Steel grade	Surface finish	Preload [kN]	$\mu_{ini,mean}$		$\mu_{act,mean}$		$\mu_{nom,mean}$		ABAQUS $\mu_s$
				Test	ABAQUS	Test	ABAQUS	Test	ABAQUS	
A_1D		1D		0.21	0.20	0.21	0.21	0.20	0.20	0.21
A_SB	1.4404	SB	M16 Bumax 88 Fp,c = 88	0.29	0.29	0.30	0.30	0.29	0.29	0.3
A_GB		GB		0.56	0.56	0.60	0.60	0.56	0.56	0.6
F_GB	1.4003	GB		0.64	0.64	0.69	0.69	0.65	0.65	0.71
D_GB	1.4462	GB		0.60	0.59	0.63	0.62	0.60	0.60	0.62
LD_GB	1.4162	GB		0.51	0.51	0.53	0.53	0.51	0.51	0.54
A1D		1D		0.20	0.19	0.20	0.20	0.19	0.19	0.2
AS	1.4404	SB	M16 Bumax 109 Fp,c = 110	0.33	0.32	0.34	0.34	0.32	0.32	0.34
AG		GB		0.58	0.57	0.65	0.64	0.57	0.57	0.64
FG	1.4003	GB		0.70	0.68	0.75	0.77	0.68	0.68	0.77
DG	1.4462	GB		0.66	0.66	0.69	0.70	0.66	0.66	0.68
LG	1.4162	GB		0.63	0.63	0.65	0.68	0.63	0.63	0.705

Note:

The clamping length  $\Sigma t = 74$  mm for M16 Bumax 88 bolts and  $\Sigma t = 77$  mm for M16 Bumax 109 bolts, the clamping length to bolt diameter ratio are therefore  $\Sigma t/d = 4.6$  and  $4.8$  respectively.

SB: short blasted, GB: grit blasted

$\mu_s$ : calibrated static coefficients of friction used in ABAQUS for the faying surface between plates, a friction coefficient of 0.5 is assumed for all other surfaces in contact

### 4.3 Parametric study

A parametric study using the calibrated numerical models for austenitic stainless steel plate with grit blasted surface finish was carried out. The effect of the hole size, bolt preload level, plate thickness and bolt size were examined.

The diameter of the normal round holes for the M16 bolts in the assembly model is 19.5 mm. In the parametric study the clearance was varied by 2 mm based on the nominal diameter therefore the three sizes studied were: 17.5, 19.5 and 21.5 mm. The influence of hole clearance on the slip factor and loss of preload is shown in Table 4. The results show that the slip factors decrease as the hole clearance increases, while the loss of preload increases. This is mainly because a larger clearance will reduce the frictional contact area under the bolt head, and therefore reduce the shear resistance of the joint ( $F_{Si}$ ).

The design bolt preload for a M16 bolt of class 10.9 is 110 kN. This preload is based on the ultimate capacity of the bolt material. A lower preload force level  $F_{p,c}^*$  based on the yield strength of the bolt material is permissible if high stresses in the bolt would lead to galling. The preload was further reduced to  $0.9 F_{p,c}^*$  to examine its effect on the slip behaviour of the joint assembly. Table 4 presents the three levels of preload used in the current parametric study and their influence on the slip resistance and loss of preload. As shown by the results, the critical slip load at 0.15 mm slip decreased with a lower level of preload in the bolt and so does the loss of preload consequently. However, slip factors increased slightly when the preload level is reduced because the rate of decrease of the preload is higher than that of the critical slip load.

The total plate thickness specified by EN 1090-2 Annex G for M16 bolts is 32 mm and the clamping length is 38 mm (assuming two 3 mm thick washers). The total thickness of the plates was increased to 48 mm and 64 mm respectively, and the corresponding clamping length increased to 54 mm and 70 mm. As shown in Table 4, the increase of plate thickness (or clamping length) led to larger nominal and initial slip factors and higher critical slip loads. The loss of preload was reduced with a longer clamping length, however this resulted in lower actual slip factors.

**Table 4 Results of parametric study: slip factor  $F_{Si}$ , slip factors and loss of preload at slip (LP)**

	hole diameter			preload level			clamping length		
	17.5 mm	19.5 mm	21.5 mm	90 kN	100 kN	110 kN	38 mm	54 mm	70 mm
$F_{Si}$ (kN)	235	231	224	203	220	235	235	251.0	251.4
$\mu_{i,ini}$	0.53	0.52	0.51	0.56	0.55	0.53	0.53	0.57	0.57
$\mu_{i,act}$	0.64	0.64	0.63	0.64	0.64	0.64	0.64	0.63	0.62
$\mu_{i,nom}$	0.54	0.53	0.51	0.56	0.55	0.54	0.54	0.57	0.57
LP	16%	18%	20%	13%	15%	16%	16%	10%	8%

Numerical models were only validated against tests results using M16 bolts. It is desirable to extend the bolt size and check the validity of the slip factors for other bolt sizes. The most commonly used bolt sizes from M12 to M36 were examined in the parametric study. It must be noted that the plate size and thickness were also modified according to the size of the bolts. As a result, the clamping length to bolt diameter ratio ( $\Sigma t/d$ ) was therefore remained equal to that specified in EN 1090-2 Annex G for M16 and M20 bolts ( $\Sigma t/d = \text{approx. } 2.3$ ). The nominal slip factors of bolt size from M12 to M36 predicted by the numerical model are presented in Fig 7. The grit blasted austenitic plates were joined by austenitic bolts in the parametric study. It can be seen that the nominal slip factors did not vary significantly which states that the slip factors obtained can be used for all size of bolts as well if the clamping length to bolt size ratio is equal to the value specified by EN1090-2 Annex G. The clamping length has an influence on the loss of preload, and therefore will affect the slip load  $F_{Si}$  as well. It is therefore desirable to used slip resistance connections with a large clamping length to bolt size ratio.

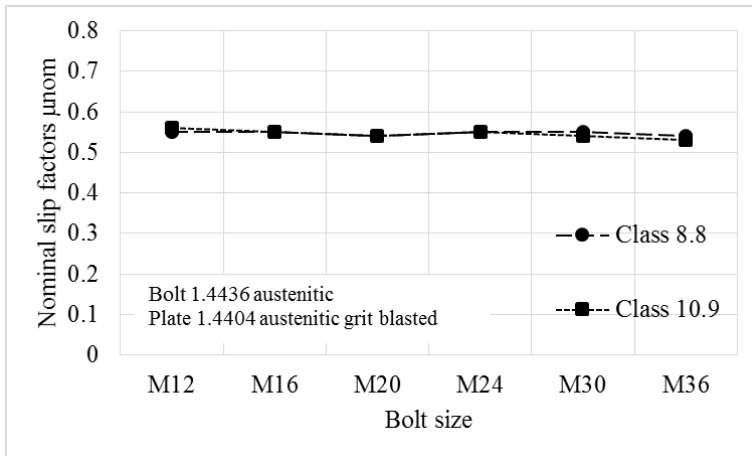


**Fig 7** Results of parametric study – varying bolt size but fixing  $\Sigma t/d = \text{approx. } 2.3$

## 5 Summary and Conclusions

Finite element models are a very convenient way to extend the range of parameters in experimental tests or to predict the behaviour of bolted connections during the whole service life of the structure. One of the most complicated modelling tasks is, however, the simulation of preloaded bolted assemblies made from viscoplastic materials such as stainless steels. Such models need a material definition that provides accurate calculation of plastic strain and associated stress in creep, relaxation and cyclic loading of the material. The present study shows that it is possible to successfully implement a comprehensive material model in the finite element calculations and carry out the parametric study.

The 2D axisymmetric model shows that the bolt load relaxation can be predicted reasonably well by the numerical model using the comprehensive material model. The 3D bolted assembly model was then calibrated and validated using slip test results. It is shown that, once calibrated with the appropriate friction coefficient, the numerical model can accurately reproduce the slip behaviour of a stainless steel slip resistant connection. A parametric study using the validated model was undertaken to examine the influence of important geometric parameters on the slip factors of a bolted assembly. The preliminary conclusions show that

- (i) Calculated slip factors are similar to those in carbon steels and confirm the findings of experiments in the SIROCO project
- (ii) The expected loss of preload is between 10% and 30%
- (iii) Higher clamping length significantly decreases the loss of preload and also improves the slip factor
- (iv) Larger holes or bolt diameters lead to a larger loss of preload

## Acknowledgements

The authors wish to express thanks to the Research Fund for Coal and Steel (RFCS)/European Commission for funding the research project "Execution and reliability of slip resistant connections for steel structures using CS and SS" SIROCO (RFSR-CT-2014-00024).

## References

- [1] Bouchaïr, A., Averseng, J., Abidelah, A., Analysis of the behaviour of stainless steel bolted connections. *Journal of Constructional Steel Research* 64(11), 2008, pp. 1264-1274.
- [2] Design Manual for Structural Stainless Steel 4th ed, P416 The Steel Construction Institute, 2017.
- [3] Kim, J., Yoon, J., Kang, B., Finite element analysis and modelling of structure with bolted joints. *Applied Mathematical Modelling* 31(5), 2007, pp. 895-911.
- [4] Manninen, T., Jakobsen, E., Pilhagen, J., Literature Study on Creep and Stress Relaxation of Stainless Steel at Room Temperature. Report to RFCS contract No. RFSR-CT-2014-00024. Outokumpu, Tornio, Finland, 2016.
- [5] Hradil, P., Sippola, M., Manninen, T., Baddoo, N., Chen, A., SIROCO report on numerical model calibration. Report to RFCS contract No. RFSR-CT-2014-00024. VTT Technical Research Centre of Finland, Espoo, Finland, 2016.
- [6] Chaboche, J.L., Rousselier, G., On the plastic and viscoplastic constitutive equations - Part I : Rules developed with internal state variable concept. *Journal of Pressure Vessel Technology* 105(1983), pp. 153–158.

- [7] Pilhagen, J. SIROCO Deliverable D5.4: Report on tensile and relaxation testing of base material and bolts. Report to RFCS contract No. RFSR-CT-2014-00024. Outokumpu, Avesta, Sweden, 2016.
- [8] Python 2.7.13 online documentation, viewed 20 July 2017, <<https://docs.python.org/2/index.html>>.
- [9] Abaqus documentation, Simulia User Assistance 2017, Dassault Systèmes, Providence, RI, USA, 2017.
- [10] Fukuoka, T., Nomura, M., Proposition of Helical Thread Modeling With Accurate Geometry and Finite Element Analysis. *Journal of Pressure Vessel Technology*, 130(2008), pp. 011204-1 - 011204-6.
- [11] EN 1090-2:2008/A1:2011, Execution of steel structures and aluminium structures, Part 2: Technical requirements for steel structures, CEN, Brussels, 2011.
- [12] EN 1990:2002/A1:2005, Eurocode - Basis of structural design, CEN, Brussels, 2005.
- [13] EN 1993-1-1:2005, Eurocode 3: Design of steel structures - Part 1-1: General rules and rules for buildings, CEN, Brussels, 2005.
- [14] EN 1993-1-4: 2006, Eurocode 3: Design of steel structures - Part 1-4: General rules - Supplementary rules for stainless steels, CEN, Brussels, 2006.
- [15] EN 14399-3:2015, High-strength structural bolting assemblies for preloading - Part 3: System HR — Hexagon bolt and nut assemblies, CEN, Brussels, 2015.
- [16] EN 14399-4:2015, High-strength structural bolting assemblies for preloading - Part 4: System HV - Hexagon bolt and nut assemblies, CEN, Brussels, 2015.
- [17] EN 14399-5:2015, High-strength structural bolting assemblies for preloading - Part 5: Plain washers, CEN, Brussels, 2015.
- [18] EN ISO 4014:2011, Hexagon head bolts. Product grades A and B, CEN, Brussels, 2011.
- [19] EN ISO 4017:2014, Fasteners. Hexagon head screws. Product grades A and B, CEN, Brussels, 2014.
- [20] EN ISO 4032:2012, Hexagon regular nuts (style 1). Product grades A and B, CEN, Brussels, 2012.
- [21] EN ISO 7091:2000, Plain washers. Normal series. Product grade C, CEN, Brussels, 2000.
- [22] EN ISO 7093-1:2000, Plain washers. Large series. Product grade A, CEN, Brussels, 2000.
- [23] Holmquist, J.L., Nadai, A., A theoretical and experimental approach to the problem of collapse of deep-well casing. *Drilling and Production Practice*, 1939, pp. 392-420.
- [24] Ramberg, W., Osgood, W.R., Technical Note No. 902: Description of stress-strain curves by three parameters. Washington, D.C., USA: National Advisory Committee for Aeronautics, 1943.
- [25] Hill, H.N., Technical Note No. 927: Determination of stress-strain relations from "offset" yield strength values. Washington, D.C., USA: National Advisory Committee for Aeronautics, 1944.
- [26] Mirambell, E., Real, E., On the calculation of deflections in structural stainless steel beams: an experimental and numerical investigation. *Journal of Constructional Steel Research*, 1(54), 2000, pp. 109-133.
- [27] Rasmussen, K.J.R., Full-range stress-strain curves for stainless steel alloys. *Journal of Constructional Steel Research*, 1(59), pp. 47-61.
- [28] Gardner, L., Ashraf, M., Structural design for non-linear metallic materials. *Engineering Structures*, 6(28), 2006, pp. 926-934.
- [29] de Vries, P., Nariman, A., Stranghöner, N., Deliverable D6.2: Slip factors for typical stainless steel surface finishes and new types of coatings for stainless steel. Report to RFCS contract No. RFSR-CT-2014-00024. Delft University of Technology, Delft, Netherlands, 2017
- [30] Nariman, A., Stranghöner, N., Deliverable D5.4: Preloading behaviour and preloading level for stainless steel bolt assemblies including relaxation with detailed specification for recommended preloading methods. Report to RFCS contract No. RFSR-CT-2014-00024. University of Duisburg-Essen, Duisburg, Germany, 2017